RESEARCH ARTICLE

The interplay between sulphur and selenium metabolism influences the intracellular redox balance in *Saccharomyces cerevisiae*

Valeria Mapelli[1], Peter R. Hillestrøm[2], Kalpesh Patil[1], Erik H. Larsen[2] & Lisbeth Olsson[1]

[1]Deparment of Chemical and Biological Engineering, Chalmers University of Technology, Göteborg, Sweden; and [2]National Food Institute, Technical University of Denmark, Søborg, Denmark

Correspondence: Valeria Mapelli, Deparment of Chemical and Biological Engineering, Chalmers University of Technology, Kemigården 4 – 41296, Göteborg, Sweden. Tel.: 0046(0)317723881; fax: 0046(0)317723801; e-mail: valeria.mapelli@chalmers.se

Received 19 April 2011; revised 19 September 2011; accepted 2 October 2011.

DOI: 10.1111/j.1567-1364.2011.00757.x

Editor: Hyun Ah Kang

Keywords
selenium; Se-metabolite profile; redox balance.

Abstract

Selenium (Se) is an essential element for most eukaryotic organisms, including humans. The balance between Se toxicity and its beneficial effects is very delicate. It has been demonstrated that a diet enriched with Se has cancer prevention potential in humans. The most popular commercial Se supplementation is selenized yeast, which is produced in a fermentation process using an inorganic source of Se. Here, we show that the uptake of Se, Se toxic effects and intracellular Se-metabolite profile are largely influenced by the level of sulphur source supplied during the fermentation. A Yap1-dependent oxidative stress response is active when yeast actively metabolizes Se, and this response is linked to the generation of intracellular redox imbalance. The redox imbalance derives from a disproportionate ratio between the reduced and oxidized forms of glutathione and also from the influence of Se metabolism on the central carbon metabolism. The observed increase in glycerol production rate, concomitant with the inhibition of ethanol formation in the presence of Se, can be ascribed to the occurrence of redox imbalance that triggers glycerol biosynthesis to replenish the pool of NAD^+.

Introduction

The boundary between toxic and beneficial concentration of selenium (Se) in nutrition is very narrow. However, Se is an essential element as it is necessary for the formation of antioxidant Se-proteins (Allan *et al.*, 1999; Burk *et al.*, 2003). In addition, enrichment of diet with supra-nutritional doses of Se has been shown to have beneficial effects in terms of cancer prevention (Clark *et al.*, 1996).

Production of selenized yeast (Larsen *et al.*, 2004; Mester *et al.*, 2006) is the most popular way to generate food supplements that can prevent Se shortage in the diet. A few studies have been carried out to optimize the production of selenized yeast (Demirci & Pometto, 1999; Demirci *et al.*, 1999), and the main problem this bioprocess has to face is the toxic effect that Se can have on yeast if Se feeding is not carefully controlled (Mapelli *et al.*, 2011).

Toxic effect of metals, such as chromium, arsenic and cadmium, has been shown to trigger a general oxidative stress response in yeast mediated by the transcription factor Yap1, which migrates to the nucleus upon activation, typically induced by oxidizing agents (Kuge *et al.*, 1997). Furthermore, these metals heavily influence sulphur (S) metabolism in yeast leading to the stimulation of glutathione (GSH) biosynthesis as means for detoxification (Vido *et al.*, 2001; Thorsen *et al.*, 2007; Pereira *et al.*, 2008). In a similar way, Se has been shown to induce a Yap1-dependent oxidative stress response via induction of *GLR1* and *TRR1* genes (Pinson *et al.*, 2000), and regeneration of GSH pool via the glutaredoxin (*GRX*) systems has been shown important in mitigating Se toxic effects (Lewinska & Bartosz, 2008).

The peculiarity of Se, compared with other metals, is its high chemical/physical similarity to S and for this reason Se-compounds follow the same metabolic routes as S-compounds (Birringer *et al.*, 2002). Therefore, Se can substitute S in amino acids and in other metabolites (Fig. 1). However, a complete substitution is not possible, owing to the higher reactivity of Se, which is also the reason for its toxicity.

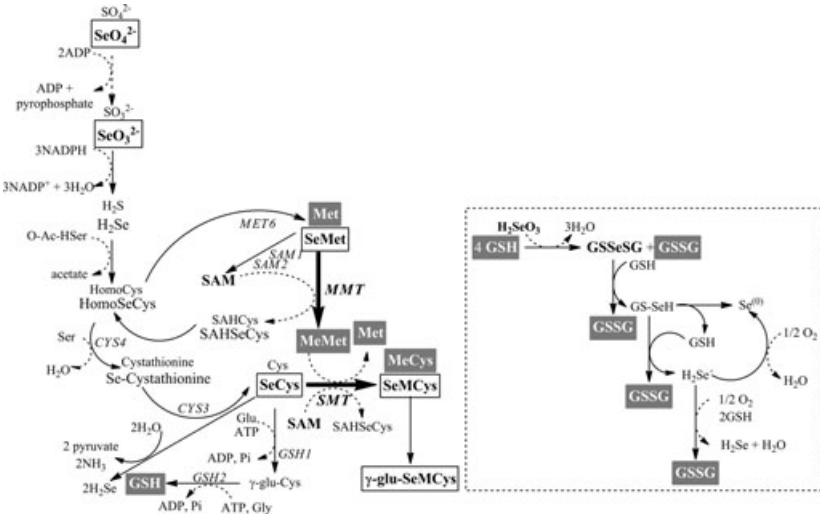

Fig. 1. Sulphur and selenium metabolism in yeast. Pathway of sulphur amino acid biosynthesis in *Saccharomyces cerevisiae* (according to Saccharomyces Genome Database www.yeastgenome.org); S-metabolites are reported with their analogous Se-metabolites. GSH reactions with Se-compounds are reported according to (Tarze *et al.*, 2007) within the dash line frame. S- and Se-metabolites that we could detect and measure are represented in a grey and white rectangular frames, respectively. GSSeSG, seleno-GSSG; SeMet, selenomethionine; SeCys, selenocysteine; SeMCys, selenomethyl-SeCys; γ-glu-SeMCys, γ-glutamyl-seleno-methylSeCys; SAM, S-adenosyl-methionine; SAHSeCys, S-adenosyl-homoSeCys.

In the prospect of optimizing the bioprocess for production of selenized yeast, it is important to understand the effects that Se has on the general cell physiology and how these effects can be tuned by the interplay between S and Se metabolism. Previous studies on metabolism and on the effects of Se on yeast have used selenite (SeO_3^{2-}) as Se source (Pinson *et al.*, 2000; Lewinska & Bartosz, 2008). In view of taking advantage of the knowledge from this work for a future production of selenized yeast, we decided to use selenate (SeO_4^{2-}) as Se source, as it is less toxic than SeO_3^{2-} (Schroeder, 1967).

Several aspects of yeast physiology in the presence of Se have been explored here, including the influence of S in determining both the efficiency of Se uptake and the intracellular Se-metabolite profile, Yap1 activation upon treatment with different Se-species and the intracellular levels and speciation of GSH upon treatment with SeO_4^{2-}. The experiments carried out in this work have shown that the interplay between S and Se metabolism is crucial in determining the toxicity levels of Se and that the macroscopic effects of Se on yeast are mainly related to redox imbalance generating upon uptake of SeO_4^{2-} by yeast.

Materials and methods

Strains, media and cultivation conditions in shake flasks

Saccharomyces cerevisiae strain used were CEN.PK113-7D (*MAT*a, *MAL2-8C* and *SUC2*) and CEN.PK113-5D (*MAT*a *ura3-52*, *MAL2-8C*, and *SUC2*), kindly provided by Dr. Peter Kötter (Biozentrum, Frankfurt, Germany). The strain expressing the recombinant gene GFP-Yap1 (*MAT*a, *MAL2-8C*, *SUC2*, *pRSGFP-YAP1*) was obtained by transformation with pRS316GFP-YAP1 (Erjavec & Nystrom, 2007), kindly provided by Dr. Mikael Molin (Gothenburg University, Gothenburg, Sweden). Growth in shake flasks was performed at 30 °C on orbital shakers at 125 r.p.m. in defined mineral medium (Verduyn *et al.*, 1992) buffered at pH 5.5 with 50 mM potassium hydrogen phthalate (Hahn-Hägerdal *et al.*, 2005) supplemented with 40 g L^{-1} glucose; here this medium is referred as S_regular (S_reg) medium. Growth under sulphur shortage condition was achieved in defined mineral medium containing 40 g L^{-1} glucose, 4.0 g L^{-1} NH_4Cl, 0.05 g L^{-1} $MgSO_4{\cdot}7H_2O$, 3.0 g L^{-1} KH_2PO_4, 0.85 g L^{-1} $MgCl_2{\cdot}6H_2O$ and buffered at pH 5.5 with 50 mM potassium hydrogen phthalate based on the study by (Boer *et al.*, 2003); vitamins and trace elements were as in (Verduyn *et al.*, 1992); this medium is also referred here as S-deficient (S_def) medium. Media for growth in shake flasks in the presence of Se were supplemented alternatively with 0.1 or 0.025 mM Na_2SeO_4; 0.1 mM Na_2SeO_3; 0.1 mM $NaHSeO_3$; or 0.1 mM SeMet.

Yeast growth conditions

For batch cultivations in bioreactors, yeast strains were grown at 30 °C in 2-L jacketed fermenters (Braun Biotech, Melsungen, Germany), and the working volume of the cultivation was 1.5 L. The pH was measured online and kept constant at 5.0 by automatic addition of 2 M KOH. Stirrer speed was 800 r.p.m., and the air flow was set at 1500 mL min^{-1}. Dissolved oxygen tension was measured online and kept above 30% of air saturation. Bioreactors were fitted with cooled condensers kept at 4 °C, and off-gas was led to a gas analyser (INNOVA; LumaSense Technologies) to measure the content of CO_2 and O_2. Chemostat cultivations were run in 1-litre reactor (DASGIP AG, Jülich, Germany) with a working volume of 0.5 L. Cultures were run with S-shortage medium supplemented with 30 g L^{-1} glucose at a dilution rate of

0.1 h^{-1}. When the steady state under S-limiting condition (also referred as to first steady state) was maintained for five volume changes, samples for analysis of mRNA and GSH levels were taken. The feeding medium was then supplemented with 0.025 mM Na_2SeO_4 (also referred as to S/Se = 8 : 1 medium) and the dilution rate was kept constant at 0.1 h^{-1}. The second steady state was reached and kept for at least three volume changes, and samples for analysis of mRNA and GSH levels in the first steady state were taken. Temperature was kept constant at 30 °C, stirrer speed was 800 r.p.m. and air flow 500 mL min^{-1}. The pH was measured online and kept constant by automatic addition of 2 M KOH with the use of DASGIP fedbatch-pro® system provided with *DASGIP Control* and Multi Pump Module MP8 (DASGIP AG). CO_2 and O_2 content in the off-gas was measured with DASGIP Off Gas analyzer GA4.

Analysis of extracellular metabolites and residual sulphate

Culture supernatants were obtained after centrifugation of samples from the fermenter at 16 000 × ***g*** at 4 °C and stored at −20 °C until analysis. Concentrations of glucose, ethanol, glycerol, acetate and pyruvate were determined by HPLC (Ultimate 3000; Dionex Corp., Sunnyvale, CA) fitted with Aminex® HPX-87H column (Bio-Rad Laboratories, Inc.) kept at 45 °C and using 5 mM H_2SO_4 as mobile phase at a flow rate of 0.6 mL min^{-1}. All compounds were detected by a refractive index detector RI-101 (Dionex Corp.) and a variable wave length detector VWD 3100 (Dionex Corp.) at a fix wavelength of 210 nm. Concentration of sulphate ions was measured by a turbidimetric method based on precipitation of sulphates as $BaSO_4$ after reacting with $BaCl_2$ under acidic conditions (Treadwell, 1924). The turbidity of the samples was measured spectrophotometrically at 550 nm, and concentration of sulphate was derived from a six-point calibration curve obtained using known concentrations of $MgSO_4$.

Analysis of intracellular S- and Se-metabolites and extracellular residual selenium

Metabolites were extracted in 100% cold methanol after quenching of yeast metabolism in cold 50% (v/v) methanol (Villas-Boas *et al.*, 2005), and the procedure was as reported in (Mapelli *et al.*, 2011). Cell-free cultivation samples were stored at −80 °C until analysis. An Agilent 1100 liquid chromatography (LC) system (Agilent, Santa Clara, USA) was used for hyphenation with the mass spectrometers for analysis of metabolites. Lyophilized metabolites were resuspended in 150 μL 0.25% formic acid (Merck KGaA, Germany) and further diluted with 0.25% formic acid before analysis with the cation-exchange system (SCX) for selenium speciation with inductively coupled plasma mass spectrometric (ICP-MS) detection and with a triple quadrupole mass spectrometry (ESI-MS/MS) detection for targeted sulphur-metabolite determination. The cation-exchange separation was achieved with an IonoSpher 5C column (150 × 2 mm, 5 μm) from Varian (Palo Alto, USA) protected with a SCX SecurityGuard (4.0 × 2.0 mm) from Phenomenex (Torrance, USA). The ICP–MS instrument used was a quadrupole-based Perkin Elmer (Glendale, Canada) Sciex Elan 6000 equipped with a dynamic reaction cell, while the triple quadrupole mass spectrometer was a Quattro Micro (Waters, Milford, USA) equipped with an ESI ion source operated in positive mode. For analysis of extracellular Se, cultivation supernatants were obtained via filtration through 22 micrometer sterile filter. An aliquot of each sample was diluted with the mobile phase and analysed in the anion-exchange system (SAX) with (ICP-MS) detection. SAX separation was hyphenated with a Perkin Elmer 200 micropump equipped with a Waters 717_{PLUS} autosampler. Separation of inorganic selenium forms was achieved with an ION-120 column (120 × 4.6 mm, 5 μm) from Transgenomic (Glasgow, UK), protected with matching guard cartridge. The outlet of the column was connected directly to the ICP-MS.

Analysis of selenium content in yeast dry biomass

Cells were harvested by centrifugation at 2500 × ***g*** for 5 min, the supernatant removed and cells washed with sterile deionized water at 2500 × ***g*** for 5 min. Biomass was freeze-dried (Christ Freeze Dryers, Beta 1–8; Montreal Biotech Inc., Dorval, Canada) and stored at −20 °C until analysis. Prior to total selenium analysis by ICP-MS, the samples were digested by concentrated nitric acid using a microwave system equipped with quartz vessels operated at a maximum pressure and temperature of 70 bar and 250 °C (Multiwave, Graz, Austria). For extraction of Se-compounds from dried biomass, 0.250 g of dried biomass were dissolved in milliQ water and exposed to ultrasonication using an ultrasonic probe Microson XL 2000 ultrasonic liquid processor (New York, USA), tip diameter 1/4″ (output 7 W for 1.5 min), and the sample extracts were further diluted before chromatographic analyses.

Determination of intracellular GSH levels

Cells were grown in shake flasks under conditions specified earlier. Cells (40 mL of culture) were harvested by

centrifugation (2500 × ***g***, 4 °C for 4 min) at 15, 30 and 60 min after addition of 0.1 mM Na_2SeO_4. The method was adapted on the basis of (Rahman *et al.*, 2007; Tan *et al.*, 2010). Cells were washed with 0.1 M potassium phosphate buffer, pH 7.4, resuspended in ice-cold 8 mM HCl, 1.3% (w/v) 5-sulfosalicylic acid solution and broken with glass beads (particle size 425–600 μm) in bead beater for 1 min at high speed. The lysate was clarified by centrifugation at 4 °C; the supernatant was used for GSH determination. Samples for di-glutathione (GSSG) determination were treated with 2-vinylpyridine for 1 h at room temperature prior to the assay. Final concentrations in the reaction mix were the following: 1.2 IU mL^{-1} GSH reductase; 0.73 mM DTNB; 0.24 mM β-NADPH; 0.09% sulphosalicylic acid. Standard curves were built using GSH and GSSG solutions, respectively, ranging between 0.206 and 26.4 μM. The assay was performed using 96-well plates with a microplate reader Fluostar (BMG Labtech GmbH, Offenburgh, Germany) reading absorbance at 405 nm after automatic addition of β-NADPH to start the reaction. Absorbance of each reaction was read every 15 s for 2 min.

GFP-Yap1 localization

Cells were grown till mid-exponential phase (OD_{600} 0.5–0.7) in shake flasks and stained with 2.5 μg mL^{-1} 4,6′ diamidino-2-phenylindole (DAPI) for 10 min at 30 °C while shaking. Cultivations were treated with indicated Se-compounds. Cultivations were sampled at different time points after treatment, and the cells were harvested by centrifugation (2500 × ***g***, 4 °C for 5 min), washed with 1 mL PBS buffer, resuspended in 50 μL of cold mounting solution of [75% (v/v) glycerol, 0.25× PBS, 200 mM diazo-bicyclooctane] and observed with a fluorescence microscope. Fluorescence microscope Leica-DMI4000B (Leica Microsystems CSM GmbH, Wetzlar, Germany) equipped with EL6000 compact light source, DFC360FX camera and controlled by LAS AF 2.0.0 software was used for fluorescence analysis. Pictures were digitally processed to enhance their quality.

Real-time quantitative PCR

Total RNA was phenol extracted as reported in (Laferté *et al.*, 2006). Samples were cleared from DNA contamination using Qiagen RNeasy Mini kit and Qiagen RNase-free DNase set (QIAGEN Nordic, Solna, Sweden), according to instruction from the manufacturer. RNA quality was determined using 2100 Bioanalyzer (Agilent Technologies) and quantified with BioPhotometer (Eppendorf, Hamburg, Germany) reading absorbance at 260 and 280 nm. RNA samples were stored at −80 °C. cDNA was synthesized from 1 μg of total RNA using RevertAid™ H Minus First Strand cDNA Synthesis kit (Fermentas, Vilnius, Lithuania) and oligo$(dT)_{18}$ primer according to instructions from the manufacturer. 100 ng of total cDNA were used in each qPCR reaction. Primers were designed with Beacon Designer Probe (Bio-Rad Laboratories, Inc.) and purchased from MWG Biotech (Ebersberg, Germany). Primer specificity was tested with melting curve analysis increasing the temperature from 60 to 95 °C using serial dilution of genomic DNA of CEN.PK113-7D or the deletion mutants *glr1*Δ, *gpd1*Δ, *gpd2*Δ and *taf10*Δ. *TAF10* was used as reference gene for relative mRNA quantification. RT-qPCR was performed in 96-well plate on a Stratagene Mx3005P instrument (Agilent Technologies) using the iScript™ One-Step RT-PCR kit with SYBR® Green (Bio-Rad Laboratories, Inc). Reactions were performed in 20-μL volume. Three technical replicates were run for each sample. At the end of the amplification, amplification specificity was verified by subjecting amplified products to melting curve analysis. The sequences of the primers used are the following: $TAF10_{fw}$ 5′-ATATTCCAGGATCAGGTCTTCCGTAGC-3′, $TAF10_{rev}$ 5′-GTAGTCTTCTCATTCTGTTGATGTTGTTG TTG-3′ (Teste *et al.*, 2009); $GLR1_{fw}$ 5′-GAACACCAAG CATTACGATTAC-3′, $GLR1_{rev}$ 5′-AGCGAGGTCAGAAGC ATAC-3′; $GPD1_{fw}$ 5′-AGGTATTCAATGTGGTGCTCTA TC-3′, $GPD1_{rev}$ 5′-GTGGAAGTAAGGTCTGTGGAAC-3′; $GPD2_{fw}$ 5′-ATTGCTATCCTCCTATGTTACTG-3′ and $GPD2_{rev}$ 5′-CATCCTTGCCATCACCTTG-3′. Threshold values were obtained using the automated settings of Mx3005P software.

Results

Sulphate presence is critical for uptake and toxicity of selenium in batch cultivations

Thanks to the very similar chemical and physical nature of S and Se, the metabolism of sulphur- and selenium-compounds is very similar and, typically, Se-metabolites are analogous to S-metabolites (Fig. 1). Therefore, we thought that uptake of Se by yeast could be influenced by S levels in the medium. Batch cultivations of the wild-type yeast strain CEN.PK113-7D were run in S_regular (S_reg) medium containing nonlimiting concentration of sulphate (SO_4^{2-}) or in S-deficient (S_def) medium, wherein SO_4^{2-} was the limiting nutrient (Boer *et al.*, 2003). The precision of the method used to measure residual sulphate in the medium is not sufficient to detect the small relative changes in sulphate concentration in S_reg medium (Fig. 2a,c); on the other hand, under sulphate deficiency, it was possible to observe that the complete depletion of sulphate was determinant in preventing

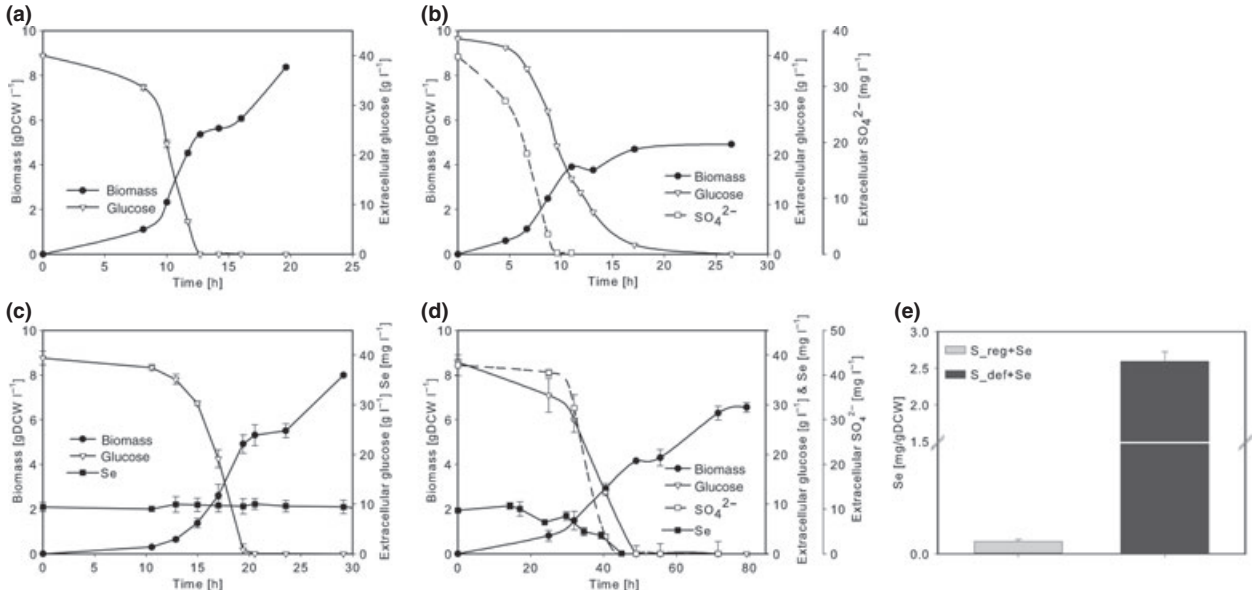

Fig. 2. Na_2SeO_4 in batch cultivations affects yeast growth and is fully consumed under S deficiency. Increase in cell biomass and residual extracellular glucose, SO_4^{2-} and Se is shown. (a) S_reg medium supplemented with 40 g L^{-1} glucose. (b) S_def medium supplemented with 40 g L^{-1} glucose. (c) S_reg medium supplemented with 40 g L^{-1} glucose and 20 mg L^{-1} Na_2SeO_4. (d) S_def medium supplemented with 40 g L^{-1} glucose and 20 mg L^{-1} Na_2SeO_4. (e) Total intracellular Se in harvested cell dry biomass, measured via ICP-MS. Data represent an average of at least three individual cultivations.

Table 1. Physiological parameters of batch cultivations

Condition	μ (h^{-1})	Y_{SX}*	Y_{SEtOH}†	Y_{SGly}‡	Y_{SAc}§	Y_{SCO2}¶	Carbon recovery (%)
S_reg	0.34 ± 0.01	0.17 ± 0.01	0.48 ± 0.01	0.05 ± 0.01	0.01 ± 0.00	0.24 ± 0.02	99 ± 1
S_reg+Se**	0.33 ± 0.01	0.16 ± 0.02	0.45 ± 0.02	0.04 ± 0.00	0.02 ± 0.00	0.23 ± 0.02	98 ± 1
S_def	0.34 ± 0.01	0.2 ± 0.03	0.49 ± 0.03	0.07 ± 0.03	0.02 ± 0.00	0.24 ± 0.02	99 ± 1
S_def + Se**	0.11 ± 0.00	0.19 ± 0.03	0.43 ± 0.05	0.14 ± 0.04	0.03 ± 0.01	0.35 ± 0.08	97 ± 3

Reported values derives from at least two biological replicates.
*Yield of biomass (C-moles/C-moles of glucose consumed).
†Yield of ethanol (C-moles/C-moles of glucose consumed).
‡Yield of glycerol (C-moles/C-moles of glucose consumed).
§Yield of acetate (C-moles/C-moles of glucose consumed).
¶Yield of CO_2 (C-moles/C-moles of glucose consumed).
**Medium containing 20 g L^{-1} Na_2SeO_4.

the further increase in biomass, although cells consumed glucose till complete depletion (Fig. 2b).

The level of extracellular sulphate was also crucial in determining to which extent the presence of Se affected yeast physiology. In particular, in the presence of 20 mg L^{-1} Na_2SeO_4, only a slight decrease of μ was observed in S_reg medium, whereas a ca. 3-fold decrease of μ was detected under sulphate deficiency (Fig. 2b,d and Table 1). Furthermore, complete uptake of Se occurred under sulphate deficiency after 45 h (Fig. 2d), while only a minimal part of the provided Se source was consumed in S_reg medium (Fig. 2c). Analysis of Se content in cell biomass demonstrated that all consumed Se was accumulated intracellularly (Fig. 2e), highlighting that the presence of excess of sulphate is drastically limiting SeO_4^{2-} uptake. Overall, we showed that Se exerts toxic effects on yeast only upon its uptake, which occurs only under sulphate deficiency.

Se-metabolite fingerprint under sulphate excess and deficiency

The intracellular Se-metabolite profile of yeast cells grown in the presence of 0.1 mM Na_2SeO_4 under S_reg and S_def condition, respectively, was studied by analysing intracellular Se-metabolites at different time points

throughout batch cultivations. Extracted metabolites were analysed via LC SCX-ICP-MS. Only organic forms of Se were considered in the analysis of the Se-metabolite fingerprint (i.e. detected residual traces of inorganic Se were excluded from the analysis). Consistently with the lower amount of intracellular Se, the total number of organic Se-species at all considered time points within exponential growth was lower in cells grown under S_reg (Fig. 3a). Interestingly, the different conditions in terms of SO_4^{2-} availability specifically affected the way in which yeast metabolized Se: the differences observed were not only related to the number of Se-species, but also to the relative amount of Se-species under the two conditions. Interestingly, SeMet (selenomethionine, metabolite 14 in Fig. 3a) was the most abundant metabolite in cells growing under S_def, but that was not the case for cells growing under S_reg, where the most abundant Se-metabolite (metabolite 19 in Fig. 3a) could not be identified. Consistently, only under S_def condition, SeMet oxide (metabolite 23 in Fig. 3a) could be detected. The differences between Se-metabolite profiles under the two conditions were further highlighted by principal component analysis (PCA) performed with Se-metabolite profiles obtained at six different time points throughout the cultivations under S_reg and S_def conditions, respectively. As shown in Fig. 3b, Se-metabolite profiles clearly separate into two clusters, whose discriminator is SO_4^{2-} levels in the growth media, and most of the variation was captured by PC1 explaining 40% of the variation. The metabolites mostly explaining this variation were metabolites 7 and 9 characterizing the S_reg condition and metabolites 22 and 23 characterizing S_def condition. PCA could not define any variation explained by time throughout the cultivations.

A few S-metabolites were also analysed and quantified. The most striking differences were shown in the levels of methionine (Met) and GSSG. In particular, the levels of Met were 2.8-fold higher in cells grown under S_reg throughout the entire exponential growth (average of six time points during exponential phase) compared to S_def, whereas GSSG showed 2.8-fold higher levels under S_def condition (data not shown).

The presence of selenium under sulphate deficiency induces a Yap1-dependent response

Generation of oxidative stress in the presence of Se-compounds is one of the possible reasons linked to toxic effects of Se (Pinson *et al.*, 2000; Lewinska & Bartosz, 2008). The transcription factor Yap1 is activated and accumulates to the nucleus upon exposure to oxidizing agents, such as H_2O_2 (Kuge & Jones, 1994; Delaunay *et al.*, 2000). To explore whether and to which extent oxidative stress was generated under the studied conditions, the yeast strain GFP-Yap1 was grown under S_reg and S_def conditions, respectively, and the effect of the addition of Na_2SeO_4 on Yap1 localization was monitored. Under our cultivation conditions, the behaviour of GFP-Yap1 upon treatment with 0.3 mM H_2O_2 was reproduced (data not shown) as reported in (Delaunay *et al.*, 2000), ensuring that the experimental setting was reliable. Addition of 0.1 mM Na_2SeO_4 to exponentially growing yeast cultures (i.e. pulse addition) strongly induced nuclear accumulation of GFP-Yap1 in cells growing under SO_4^{2-} deficiency, whereas no translocation of GFP-Yap1 to the nucleus was detected in cells growing under S_reg condition (Fig. 4a). The nuclear localization of GFP-Yap1 was detected after 5 min from the addition of Na_2SeO_4 and sustained for at least 90 min (Fig. 4a). GFP-Yap1 nuclear localization was also induced upon pulse addition of lower Na_2SeO_4 concentration (i.e. 0.025 mM Na_2SeO_4), although it occurred only after 30 min (data not shown) under S_def. Exponentially growing cells that had been cultured in the constant presence of 0.1 or 0.025 mM Na_2SeO_4 did not show any nuclear accumulation of GFP-Yap1 under SO_4^{2-} excess and only weak signal (data not shown) of nuclear accumulation was detectable under SO_4^{2-} deficiency (i.e. only a very small fraction of cells displayed nuclear GFP fluorescence) if compared with the signal observed few minutes after the pulse addition of Na_2SeO_4 to exponentially growing cells (Fig. 4a). Therefore, high levels of SO_4^{2-} prevented Se toxicity by preventing selenate uptake. Such toxicity was clearly linked to the generation of oxidizing intracellular environment that triggered a Yap1-dependent response. Further and more direct validation of a Yap1-dependent oxidative stress response triggered by the presence of Na_2SeO_4 under S_def conditions was shown by the dramatic increase of *GLR1* (i.e. GSH oxidoreductase, which is known to be among Yap1-regulons) (Lee *et al.*, 1999; Grant, 2001) transcript levels upon 30-min incubation in the presence of 0.1 mM Na_2SeO_4 (Fig. 4b).

The specific form of selenium is critical for induction of Yap1-dependent response

As different forms of Se follow specific metabolic routes, their effects on yeast physiology might greatly vary. We monitored the behaviour of GFP-Yap1 in the presence of Se-compounds different from Na_2SeO_4 and observed that 0.1 mM SeMet added to exponentially growing cells under SO_4^{2-} deficiency induced GFP-Yap1 nuclear accumulation only after 30 min after its addition (Fig. 4c). On the other hand, neither 0.1 mM Na_2SeO_3 nor 0.1 mM $NaHSeO_3$ induced GFP-Yap1 nuclear

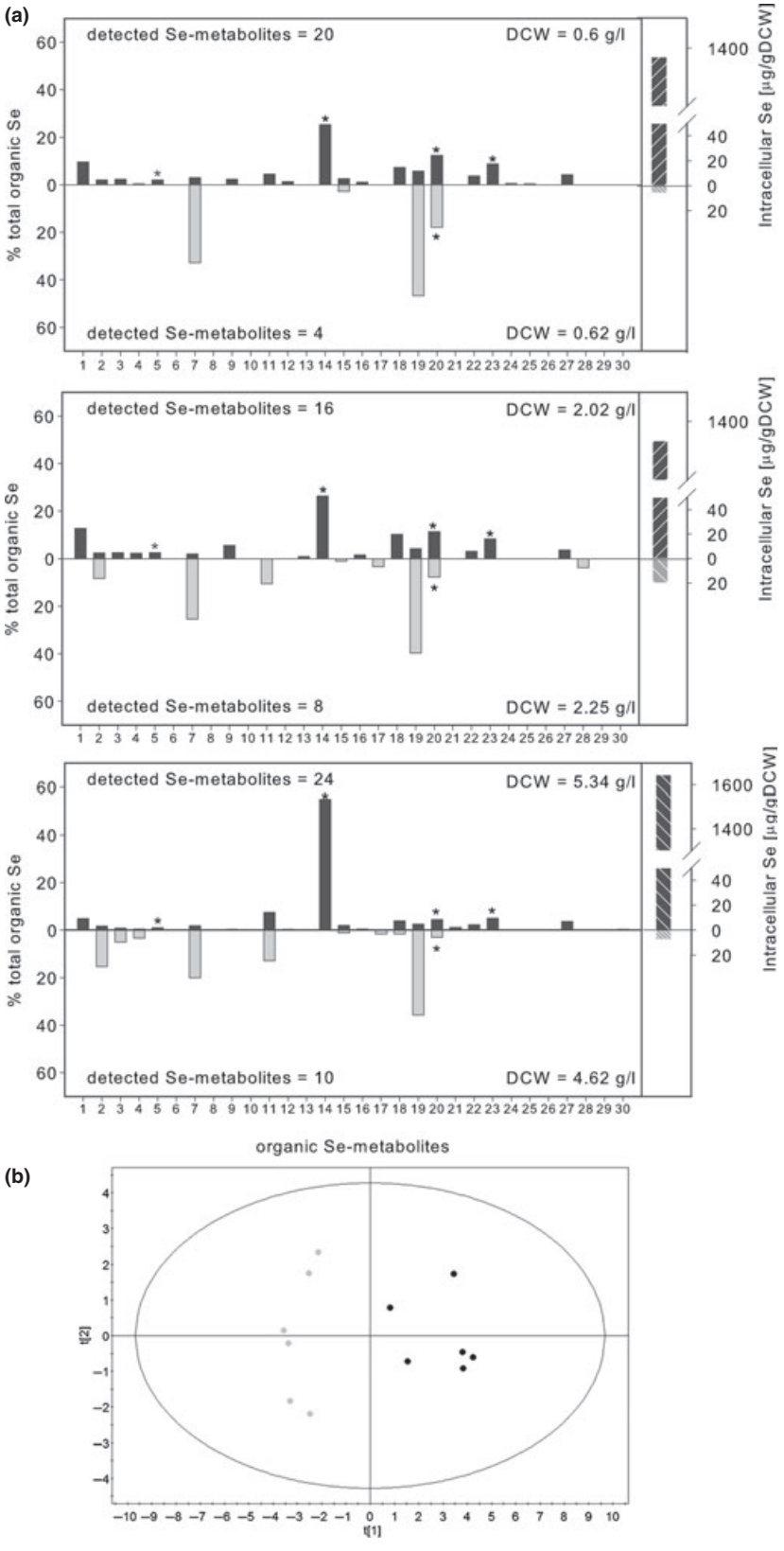

Fig. 3. Comparison of intracellular total S- and Se-metabolite profile between S_reg and S_def condition supplemented with 20 mg L^{-1} Na_2SeO_4. (a) Numbers represent corresponding peaks in the chromatograms obtained via SCX-ICP-MS analysis of intracellular Se-metabolites. The area of each peak has been measured and normalized on the total peak area of each chromatogram. The amount of each peak is then reported as percentage of all organic Se-compounds detected. Black bars represent Se-metabolites under S_def condition supplemented with 20 mg L^{-1} Na_2SeO_4; grey bars represent Se-metabolites under S_reg condition supplemented with 20 mg L^{-1} Na_2SeO_4. Each plot represents a specific time point during batch cultivations and the comparison S_reg vs. S_def is between time points with similar value of biomass (reported as DCW L^{-1} in each corresponding panel). On the right end of each plot, the dashed vertical bars represent the total amount of Se (µg Se per g DCW) accumulated in yeast biomass at the corresponding time points. Peaks identified are 5, γ-glutamyl-seleno-methylselenocysteine; 14, SeMet; 20, Se-GSSG; 23, SeMet oxide. (b) PCA of Se-metabolite profiles under S_reg (grey dots) and S_def (black dots) conditions supplemented with 20 mg L^{-1} Na_2SeO_4, respectively. Each dot represents a single metabolite profile at a specific time point during the cultivations. Each time point has been sampled twice for Se-metabolite profile analysis.

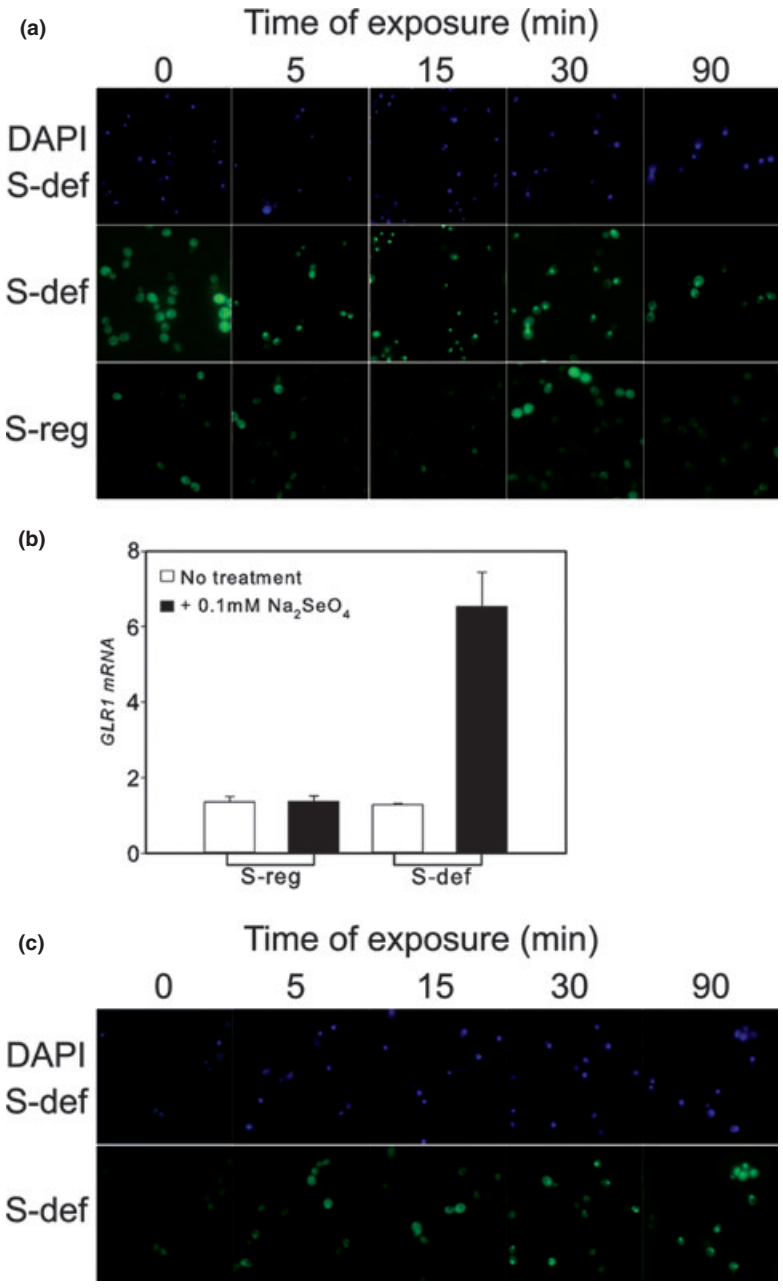

Fig. 4. Yap1 localization after exposure to Na_2SeO_4 and SeMet under S_reg and S_def conditions. (a) Exponentially growing cells were treated with 0.1 mM Na_2SeO_4, and GFP-Yap1 localization was monitored at indicated time points after treatment. Time 0 is before treatment. Each sample was also stained with DAPI to localize cell nuclei. (b) *GLR1* mRNA levels measured via qPCR in cells exponentially growing under the indicated conditions, before treatment (white bars) and after 30 min exposure to 0.1 mM Na_2SeO_4 (black bars). Results are representative of three biological replicates. (c) Exponentially growing cells under the indicated conditions were treated with 0.1 mM SeMet, and GFP-Yap1 localization was monitored at indicated time points. Pictures showed are representative of results obtained in two biological replicates.

accumulation under S_reg and S_def conditions, respectively (data not shown).

Intracellular GSH levels are influenced by the presence of selenate under sulphate deficiency

Induction of genes coding for GSH-related enzymes, such as GSH reductase (*GLR1*) and GSH-dependent redox enzymes (glutaredoxins, *GRX*), in response to selenite has been previously described (Pinson *et al.*, 2000; Lewinska & Bartosz, 2008). It has also been proposed that oxidative stress generation in cells growing in the presence of selenium might be due to intracellular redox imbalance linked to a disproportionate ratio between the reduced form of GSH and the oxidized one (GSSG) (Tarze *et al.*, 2007). As we proved that the addition of Na_2SeO_4 to yeast cultivations growing under sulphate deficiency triggered an oxidative stress response through activation of Yap1, we investigated whether the imbalance of GSH species might also be involved. Yeast cultivations in the exponential growth phase were treated with 0.1 mM Na_2SeO_4, and the level of total GSH and GSSG were

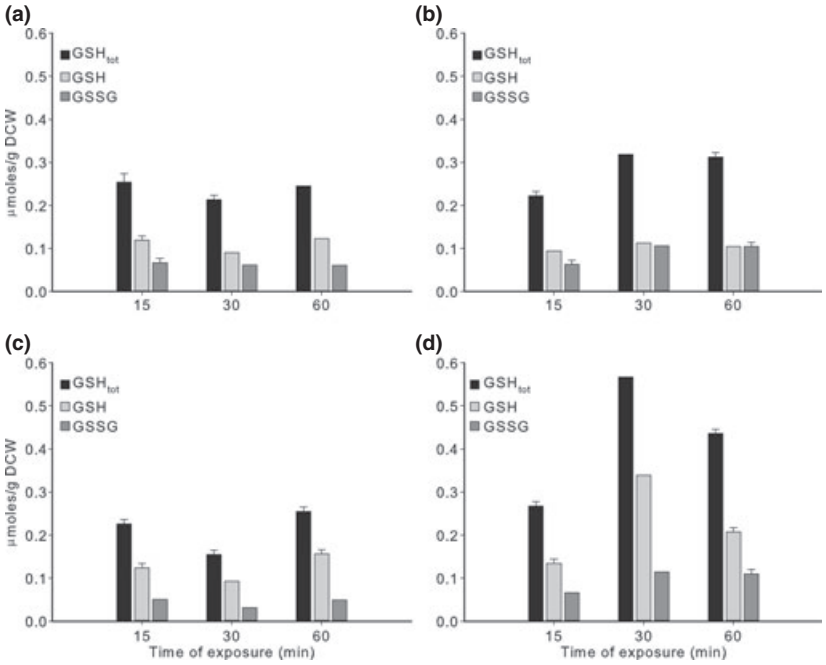

Fig. 5. Intracellular GSH levels measured after exposure to Na_2SeO_4. Exponentially growing cells were treated with Na_2SeO_4, and the levels of total GSH (GSH_{tot}) and GSSG were measured at the indicated time points after addition of 0.1 mM Na_2SeO_4. Owing to the conditions of the assay, levels of GSH were calculated according to: $[GSH]_{tot} = [GSH] + 2 \cdot [GSSG]$. (a) S_reg nontreated; (b) S_reg + Na_2SeO_4; (c) S_def nontreated (d) S_def + Na_2SeO_4. Data represent an average of two biological replicates; two technical replicates were performed for each biological replicates.

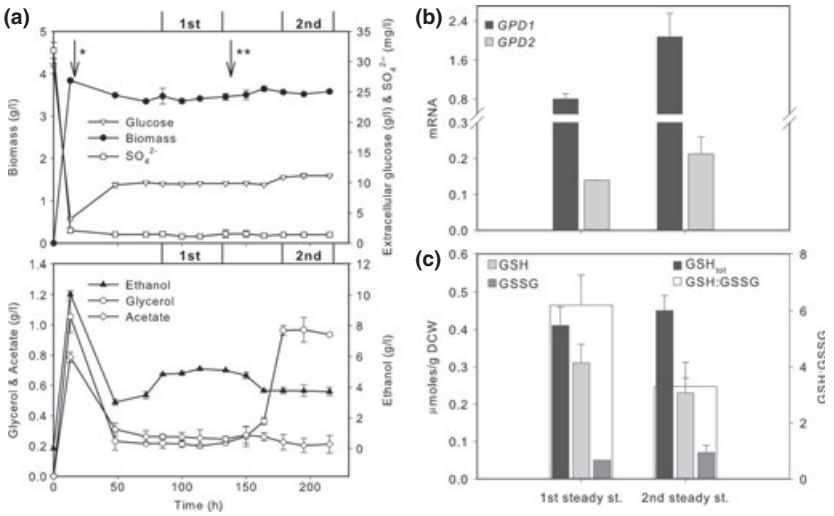

Fig. 6. Sulphate-limited continuous cultivations. (a) Profiles of cell biomass and extracellular metabolites throughout the cultivation. Arrow marked with * indicates the time point when S-limited feed was started after the batch phase; arrow marked with ** indicates when Na_2SeO_4 was added to the feed. The time intervals marked as first and second indicate the first steady state under S-limitation and the second steady state reached after addition of Na_2SeO_4 (S/Se ratio = 8 : 1), respectively. (b) mRNA levels of *GPD1* and *GPD2* obtained via qPCR and related to first and second steady state of sulphate-limited cultivations. (c) Intracellular GSH levels and calculated GSH/GSSG ratio in the first steady state and second steady state of sulphate-limited cultivations. Data represent the average from at least three individual cultivations.

determined, respectively (Rahman *et al.*, 2007) (Fig. 5a–d). Consistently with Yap1 activation data, we observed major changes in GSH levels in cultivations treated with Na_2SeO_4 only under SO_4^{2-} deficiency (Fig. 5d), wherein total GSH reached ~0.6 µmoles g^{-1} dry cell weight (DCW), while no significant changes were detected under SO_4^{2-} excess after treatment with Na_2SeO_4 and total GSH levels were found to be stable at ~0.25 µmoles g^{-1} DCW (Fig. 5c). Levels of intracellular GSH in cells growing under S_reg and S_def, respectively, treated with 0.3 mM H_2O_2 did not show any significant change (data not shown). Interestingly, although the nuclear accumulation

Table 2. Physiological parameters of chemostat cultivations

Bioprocess phase	Y_{SX}*	$r_{glucose}$†	$r_{biomass}$‡	$r_{ethanol}$§	$r_{glycerol}$¶	$r_{acetate}$**	r_{CO2}††	RQ‡‡
1st steady state§§	0.21 ± 0.00	19.7 ± 0.1	4.1 ± 0.0	6.4 ± 0.5	0.2 ± 0.0	0.1 ± 0.0	6.5 ± 0.3	1.5 ± 0.1
2nd steady state¶¶	0.25 ± 0.01	16.6 ± 0.5	4.1 ± 0.0	3.8 ± 0.2	0.8 ± 0.1	0.1 ± 0.0	6.2 ± 0.1	1.3 ± 0.1

Reported values are based on at least three biological replicates.
*Yield of biomass (C-moles/C-moles of glucose consumed).
†Specific rate of glucose consumption (C-mmoles consumed glucose g DCW^{-1} h^{-1}).
‡Specific rate of biomass production (C-mmoles biomass g DCW^{-1} h^{-1}).
§Specific rate of ethanol production (C-mmoles ethanol g DCW^{-1} h^{-1}).
¶Specific rate of glycerol production (C-mmoles glycerol g DCW^{-1} h^{-1}).
**Specific rate of acetate production (C-mmoles acetate g DCW^{-1} h^{-1}).
††Specific rate of carbon dioxide production (C-mmoles CO_2 g DCW^{-1} h^{-1}).
‡‡Respiratory quotient calculated in real time during bioprocess.
§§Steady state under sulphate limitation.
¶¶Steady state under sulphate limitation and Se/S ratio equal to 1 : 10.

of Yap1 was detectable already 15 min after treatment with Na_2SeO_4, significant increase in GSH levels were observed only 30 min after treatment. The calculated ratio GSH/GSSG showed an increase at 30 min after treatment with Na_2SeO_4 under S_def condition, but such change could not be considered significant owing to high standard deviation. Therefore, our data could not demonstrate any statistically significant redox imbalance owing to a disproportionate GSH/GSSG ratio.

The rate of glycerol production increases in the presence of selenium under sulphate limitation

To better determine the effects of selenium intake on yeast metabolism, we set up continuous cultivations that allowed for determination of specific rates under well-defined environmental conditions. The rate limiting substrate of our cultivations was sulphate (S-limited). Once the cultivation reached the steady state, Na_2SeO_4 was added to the feeding medium and a second steady state was established. Physiological parameters were measured throughout the entire cultivation, and samples of the first- and second steady state for RNA and GSH extraction were taken after at least three residence times. Three different concentrations of Na_2SeO_4 were added to the S-limited medium resulting in S/Se molar ratio equal to 1 : 1, 8 : 1 and 12 : 1, respectively. Under S/Se ratio equal to 1 : 1, biomass washout occurred, which could be attributed to toxic effects and growth inhibition owing to high selenium levels (data not shown), whereas the steady state was reached under both 8 : 1 (Fig. 6) and 12 : 1 (data not shown). The comparison of physiological parameters between the two steady states clearly shows that after addition of Na_2SeO_4, major changes occurred in the specific production rate of glycerol and ethanol with a 4-fold increase and 1.7-fold decrease, respectively (Table 2). The specific production rate of biomass did not change, while glucose consumption rate in the second steady state slightly decreased after the addition of Na_2SeO_4 (Table 2).

To determine whether the increase in glycerol production rate was related to the increase in expression of *GPD1* and *GPD2* genes (Eriksson *et al.*, 1995), the transcription levels of these two genes were measured via qPCR (Fig. 6b). Transcript levels of both *GPD1* and *GPD2* increased in the second steady state under S/Se ratio equal to 8 : 1 with a fold increase of 2.2 for *GPD1* and 1.5 for *GPD2*. Therefore, the higher glycerol levels in the second steady state were consistently related to increased expression of the two main responsible genes for glycerol biosynthesis.

In contrast to data observed in shake flask cultivations (Fig. 5), the measurement of intracellular GSH species within the two steady states showed that, although total GSH levels did not change, there was a significant change of GSH/GSSG ratio (Fig. 6c), decreasing from 6.2 (first steady state) to 3.3 (second steady state).

Discussion

The analogies between selenium and sulphur metabolism have been demonstrated by the fact that all small organic Se-compounds in plants, yeasts, bacteria or animals are isologues of sulphur compounds, and the enzymes involved in sulphate metabolism and in the transsulphuration pathway typically do not discriminate between S- and Se-compounds (Birringer *et al.*, 2002).

Results presented here show that selenate (SeO_4^{2-}) uptake by yeast is strictly dependent on the levels of sulphate (SO_4^{2-}) in the medium, as only under SO_4^{2-} deficiency SeO_4^{2-} is fully internalized and metabolized by yeast. A few studies have shown the presence of transport

systems specific for uptake of selenite (SeO_3^{2-}) in yeast (Lazard *et al.*, 2010; McDermott *et al.*, 2010). While no detailed molecular studies have been carried out to identify a specific SeO_4^{2-} transport mechanism, it is likely that Sul1 and Sul2 permeases active in SO_4^{2-} uptake are also responsible for uptake of SeO_4^{2-} (Cherest *et al.*, 1997), as it occurs in *Arabidopsis thaliana* (Barberon *et al.*, 2008). Also our data support this conclusion.

Owing to the tight interplay between S and Se metabolism, it might appear rather obvious that they exert reciprocal influence on each other. However, it is very interesting to observe that the Se-metabolite profile is highly influenced by the SO_4^{2-} availability: S_reg and S_def conditions influenced the amount of incorporated Se, but most surprisingly the intracellular Se speciation was also highly affected. In particular, SeMet, which is typically the major organic form of Se in yeast (Ip *et al.*, 2000; Larsen *et al.*, 2004), represents the main Se-metabolite only under S_def condition, while other Se-species are relatively more abundant under S_reg condition. Accordingly, the levels of methionine are higher under S_reg conditions, wherein the very low levels of intracellular Se do not effectively compete with sulphur.

More detailed Se-metabolite profiles have been obtained concerning the study of Se speciation in selenized yeast (Dernovics *et al.*, 2009), but only little information derives from comparative studies carried out to define how Se-metabolite profile is influenced by different cultivation conditions (Rao *et al.*, 2010). The coupling of comparative studies with high sensitive technology for identification of the complete Se-metabolome would allow elucidation of the interplay between S and Se metabolism and optimization of fermentation processes for the production of selenized yeast.

Previous studies have indicated that Na_2SeO_3 triggers the typical oxidative stress response by inducing the transcription of specific genes controlled by transcriptional factors responsive to oxidative stress (Salin *et al.*, 2008). In particular, Yap1-dependent induction of both GSH reductase *GLR1* and thioredoxin reductase *TRR1* has been demonstrated after treatment of cells with selenite (Pinson *et al.*, 2000). Here, we show that a rapid Yap1 activation occurs only under S_def condition upon treatment with Na_2SeO_4, which is also responsible for the strong induction of *GLR1* expression. Interestingly, we noticed that the effect on Yap1 activation is highly dependent on the Se form supplied. Surprisingly, no Yap1 nuclear accumulation could be detected after treatment with Na_2SeO_3. Such discrepancy with previous results (Pinson *et al.*, 2000) might be linked to the different experimental set-up and the amount of Na_2SeO_3 used (i.e. 0.1 mM in our case and 10 mM in (Pinson *et al.*, 2000). In addition, the metabolism of SeO_4^{2-} requires the consumption of 2 moles ATP per 1 mole SeO_4^{2-} (Fig. 1) that is not required for SeO_3^{2-} metabolism (SGD project. 'Saccharomyces Genome Database' http://www.yeastgenome.org/). Such energetic requirement is further increased if we consider that the treatment with Na_2SeO_4 under S_def resulted in higher levels of GSH, whose biosynthesis requires 2 moles ATP per 1 mole GSH (Fig. 1).

As ATP biosynthesis through glycolysis is strictly connected to NADH production, it implies that the general redox balance determined by NADH/NAD^+ ratio is different in cells treated with SeO_4^{2-} than with SeO_3^{2-} and is likely influencing the oxidative stress response. The effect of SeO_4^{2-} on NADH/NAD^+ redox balance can also be inferred from the fourfold increase in the glycerol-specific production rate occurring in the continuous cultivations after addition of SeO_4^{2-} to the feed. Increase in glycerol formation is a typical response of yeast to diverse stress conditions (Blomberg & Adler, 1989; Izawa *et al.*, 2004; Berovic & Herga, 2007) and is also required as redox sink for excess of cytosolic NADH (Ansell *et al.*, 1997). This metabolic route exploited by yeast to regenerate the NAD^+ pool is especially active under anaerobic conditions and is *GPD2* dependent (Ansell *et al.*, 1997). Under aerobic conditions, the same response is observable in cells treated with sulphite (SO_3^{2-}), which inhibits the reduction of acetaldehyde to ethanol, thus preventing the oxidation of NADH to NAD^+ (Neuberg, 1946; Ansell *et al.*, 1997). Interestingly, in S-limited continuous cultivations, we showed a clear decrease in ethanol production rate concomitant with the increase in glycerol production rate when cells were growing in the presence of Na_2SeO_4. We propose that the highly reactive SeO_3^{2-} forming upon SeO_4^{2-} metabolism might act as SO_3^{2-}, blocking acetaldehyde reduction to ethanol and thus triggering the production of glycerol via induction of *GPD1* and *GPD2* expression.

GSH is known to be a key factor in cell defence against oxidative stress and metal toxicity (Grant, 2001; Pompella *et al.*, 2003). Na_2SeO_4 treatment of cells growing in shake flask under S_def caused a general increase in intracellular total GSH, which is consistent with the observed activation of Yap1, as *GSH1* transcription is Yap1 dependent (Wheeler *et al.*, 2003).

The increase in GSH levels was not clearly visible in cells growing in the presence of Na_2SeO_4 in continuous cultivations; most probably, because under steady-state conditions, the outcome we observe is the balance between a continuous conversion of GSH to GSSG and a continuous biosynthesis of GSH to cope against GSH depletion. However, the GSH/GSSG ratio definitely decreased in continuous cultivations after addition of Na_2SeO_4. This change is ascribable to spontaneous reactions occurring between GSH and SeO_3^{2-}, shifting the

balance towards GSSG synthesis (Fig. 1) (Tarze *et al.*, 2007).

In conclusion, here we show several yeast physiological aspects that are affected upon growth in the presence of selenate, and also, we demonstrate that the presence of sulphate is critical in determining to which extent Se induces metabolic changes in yeast. SeO_4^{2-} induces a prompt Yap1 induction most probably linked to the generation of an intracellular oxidizing environment, which can be inferred also by the presence of higher GSH levels after SeO_4^{2-} treatment. Furthermore, the higher specific production rate of glycerol suggests that such oxidizing environment is related to a general redox imbalance possibly deriving from an enhanced NADH/NAD^+ ratio. The information gathered in this work can be taken into consideration when implementing a bioprocess for production of selenized yeast. In fact, knowing how the interplay between sulphur and selenium metabolism acts on the Se-metabolite profile can allow a better definition of process conditions to rationally tune Se-metabolic routes in yeast.

Acknowledgments

The authors thank Dr. Mikael Molin (Gothenburg University, Gothenburg, Sweden) for providing the plasmid pRS316GFP-YAP1, for his assistance in qPCR experiments and scientific discussions; the authors also thank all the partners of the YESSEL project for very fruitful discussions throughout the ongoing project. This research was financed by The Danish Research Agency via the YESSEL project 'Biosynthesis of cancer preventive organoselenium compounds by metabolically engineered yeast'.

References

Allan CB, Lacourciere GM & Stadtman TC (1999) Responsiveness of selenoproteins to dietary selenium. *Annu Rev Nutr* **19**: 1–16.

Ansell R, Granath K, Hohmann S, Thevelein JM & Adler L (1997) The two isoenzymes for yeast NAD+-dependent glycerol 3-phosphate dehydrogenase encoded by GPD1 and GPD2 have distinct roles in osmoadaptation and redox regulation. *EMBO J* **16**: 2179–2187.

Barberon M, Berthomieu P, Clairotte M, Shibagaki N, Davidian JC & Gosti F (2008) Unequal functional redundancy between the two *Arabidopsis thaliana* high-affinity sulphate transporters SULTR1;1 and SULTR1;2. *New Phytol* **180**: 608–619.

Berovic M & Herga M (2007) Heat shock on *Saccharomyces cerevisiae* inoculum increases glycerol production in wine fermentation. *Biotechnol Lett* **29**: 891–894.

Birringer M, Pilawa S & Flohe L (2002) Trends in selenium biochemistry. *Nat Prod Rep* **19**: 693–718.

Blomberg A & Adler L (1989) Roles of glycerol and glycerol-3-phosphate dehydrogenase (NAD+) in acquired osmotolerance of *Saccharomyces cerevisiae*. *J Bacteriol* **171**: 1087–1092.

Boer VM, de Winde JH, Pronk JT & Piper MD (2003) The genome-wide transcriptional responses of *Saccharomyces cerevisiae* grown on glucose in aerobic chemostat cultures limited for carbon, nitrogen, phosphorus, or sulfur. *J Biol Chem* **278**: 3265–3274.

Burk RF, Hill KE & Motley AK (2003) Selenoprotein metabolism and function: evidence for more than one function for selenoprotein P. *J Nutr* **133**: 1517S–1520S.

Cherest H, Davidian JC, Thomas D, Benes V, Ansorge W & Surdin-Kerjan Y (1997) Molecular characterization of two high affinity sulfate transporters in *Saccharomyces cerevisiae*. *Genetics* **145**: 627–635.

Clark LC, Combs GF Jr, Turnbull BW *et al.* (1996) Effects of selenium supplementation for cancer prevention in patients with carcinoma of the skin. A randomized controlled trial. Nutritional Prevention of Cancer Study Group. *JAMA* **276**: 1957–1963.

Delaunay A, Isnard A-D & Toledano MB (2000) H2O2 sensing through oxidation of the Yap1 transcription factor. *EMBO J* **19**: 5157–5166.

Demirci A & Pometto AL III (1999) Production of organically bound selenium yeast by continuous fermentation. *J Agric Food Chem* **47**: 2491–2495.

Demirci A, Pometto AL III & Cox DJ (1999) Enhanced organically bound selenium yeast production by fed-batch fermentation. *J Agric Food Chem* **47**: 2496–2500.

Dernovics M, Far J & Lobinski R (2009) Identification of anionic selenium species in Se-rich yeast by electrospray QTOF MS/MS and hybrid linear ion trap/orbitrap MS. *Metallomics* **1**: 317–329.

Eriksson P, Andre L, Ansell R, Blomberg A & Adler L (1995) Cloning and characterization of GPD2, a second gene encoding sn-glycerol 3-phosphate dehydrogenase (NAD+) in *Saccharomyces cerevisiae*, and its comparison with GPD1. *Mol Microbiol* **17**: 95–107.

Erjavec N & Nystrom T (2007) Sir2p-dependent protein segregation gives rise to a superior reactive oxygen species management in the progeny of *Saccharomyces cerevisiae*. *P Natl Acad Sci USA* **104**: 10877–10881.

Grant CM (2001) Role of the glutathione/glutaredoxin and thioredoxin systems in yeast growth and response to stress conditions. *Mol Microbiol* **39**: 533–541.

Hahn-Hägerdal B, Karhumaa K, Larsson CU, Gorwa-Grauslund M, Gorgens J & van Zyl WH (2005) Role of cultivation media in the development of yeast strains for large scale industrial use. *Microb Cell Fact* **4**: 31.

Ip C, Birringer M, Block E, Kotrebai M, Tyson JF, Uden PC & Lisk DJ (2000) Chemical speciation influences comparative activity of selenium-enriched garlic and yeast in mammary cancer prevention. *J Agric Food Chem* **48**: 4452.

Izawa S, Sato M, Yokoigawa K & Inoue Y (2004) Intracellular glycerol influences resistance to freeze stress in

Saccharomyces cerevisiae: analysis of a quadruple mutant in glycerol dehydrogenase genes and glycerol-enriched cells. *Appl Microbiol Biotechnol* **66**: 108–114.

Kuge S & Jones N (1994) YAP1 dependent activation of TRX2 is essential for the response of *Saccharomyces cerevisiae* to oxidative stress by hydroperoxides. *EMBO J* **13**: 655–664.

Kuge S, Jones N & Nomoto A (1997) Regulation of yAP-1 nuclear localization in response to oxidative stress. *EMBO J* **16**: 1710–1720.

Laferté A, Favry E, Sentenac A, Riva M, Carles C & Chedin S (2006) The transcriptional activity of RNA polymerase I is a key determinant for the level of all ribosome components. *Genes Dev* **20**: 2030–2040.

Larsen EH, Hansen M, Paulin H, Moesgaard S, Reid M & Rayman M (2004) Speciation and bioavailability of selenium in yeast-based intervention agents used in cancer chemoprevention studies. *J AOAC Int* **87**: 225–232.

Lazard M, Blanquet S, Fisicaro P, Labarraque G & Plateau P (2010) Uptake of selenite by *Saccharomyces cerevisiae* involves the high and low affinity orthophosphate transporters. *J Biol Chem* **285**: 32029–32037.

Lee J, Godon C, Lagniel G, Spector D, Garin J, Labarre J & Toledano MB (1999) Yap1 and Skn7 control two specialized oxidative stress response regulons in yeast. *J Biol Chem* **274**: 16040–16046.

Lewinska A & Bartosz G (2008) A role for yeast glutaredoxin genes in selenite-mediated oxidative stress. *Fungal Genet Biol* **45**: 1182–1187.

Mapelli V, Hillestrom PR, Kapolna E, Larsen EH & Olsson L (2011) Metabolic and bioprocess engineering for production of selenized yeast with increased content of seleno-methylselenocysteine. *Metab Eng* **13**: 282–293.

McDermott JR, Rosen BP & Liu Z (2010) Jen1p: a high affinity selenite transporter in yeast. *Mol Biol Cell* **21**: 3934–3941.

Mester Z, Willie S, Yang L *et al.* (2006) Certification of a new selenized yeast reference material (SELM-1) for methionine, selenomethinone and total selenium content and its use in an intercomparison exercise for quantifying these analytes. *Anal Bioanal Chem* **385**: 168–180.

Neuberg C (1946) The biochemistry of yeast. *Annu Rev Biochem* **15**: 435–474.

Pereira Y, Lagniel G, Godat E, Baudouin-Cornu P, Junot C & Labarre J (2008) Chromate causes sulfur starvation in yeast. *Toxicol Sci* **106**: 400–412.

Pinson B, Sagot I & Daignan-Fornier B (2000) Identification of genes affecting selenite toxicity and resistance in *Saccharomyces cerevisiae*. *Mol Microbiol* **36**: 679–687.

Pompella A, Visvikis A, Paolicchi A, De Tata V & Casini AF (2003) The changing faces of glutathione, a cellular protagonist. *Biochem Pharmacol* **66**: 1499–1503.

Rahman I, Kode A & Biswas SK (2007) Assay for quantitative determination of glutathione and glutathione disulfide levels using enzymatic recycling method. *Nat Protoc* **1**: 3159–3165.

Rao Y, McCooeye M, Windust A, Bramanti E, D'Ulivo A & Mester Z (2010) Mapping of selenium metabolic pathway in yeast by liquid chromatography-Orbitrap mass spectrometry. *Anal Chem* **82**: 8121–8130.

Salin H, Fardeau V, Piccini E *et al.* (2008) Structure and properties of transcriptional networks driving selenite stress response in yeasts. *BMC Genomics* **9**: 333.

Schroeder HA (1967) Effects of selenate, selenite and tellurite on the growth and early survival of mice and rats. *J Nutr* **92**: 334–338.

Tan SX, Greetham D, Raeth S, Grant CM, Dawes IW & Perrone GG (2010) The thioredoxin-thioredoxin reductase system can function in vivo as an alternative system to reduce oxidized glutathione in *Saccharomyces cerevisiae*. *J Biol Chem* **285**: 6118–6126.

Tarze A, Dauplais M, Grigoras I *et al.* (2007) Extracellular production of hydrogen selenide accounts for thiol-assisted toxicity of selenite against *Saccharomyces cerevisiae*. *J Biol Chem* **282**: 8759–8767.

Teste MA, Duquenne M, Francois JM & Parrou JL (2009) Validation of reference genes for quantitative expression analysis by real-time RT-PCR in *Saccharomyces cerevisiae*. *BMC Mol Biol* **10**: 99.

Thorsen M, Lagniel G, Kristiansson E, Junot C, Nerman O, Labarre J & Tamas MJ (2007) Quantitative transcriptome, proteome, and sulfur metabolite profiling of the *Saccharomyces cerevisiae* response to arsenite. *Physiol Genomics* **30**: 35–43.

Treadwell FP (1924) *Analytical Chemistry*. John Wiley and Son, New York.

Verduyn C, Postma E, Scheffers WA & Van Dijken JP (1992) Effect of benzoic acid on metabolic fluxes in yeasts: a continuous-culture study on the regulation of respiration and alcoholic fermentation. *Yeast* **8**: 501–517.

Vido K, Spector D, Lagniel G, Lopez S, Toledano MB & Labarre J (2001) A proteome analysis of the cadmium response in *Saccharomyces cerevisiae*. *J Biol Chem* **276**: 8469–8474.

Villas-Boas SG, Mas S, Akesson M, Smedsgaard J & Nielsen J (2005) Mass spectrometry in metabolome analysis. *Mass Spectrom Rev* **24**: 613–646.

Wheeler GL, Trotter EW, Dawes IW & Grant CM (2003) Coupling of the transcriptional regulation of glutathione biosynthesis to the availability of glutathione and methionine via the Met4 and Yap1 transcription factors. *J Biol Chem* **278**: 49920–49928.